Double-Dwell Hybrid Acquisition in DS-UWB System

YuPeng Wang* *Associate Member*, KyungHi Chang* *Lifelong Member*

ABSTRACT

In this paper, we analyze the performance of double-dwell hybrid initial acquisition in DS-UWB system via detection, miss, false alarm probabilities and mean acquisition time. In the analysis, we consider the effect of the acquisition sequence, and deployment scenario of the abundant multipath components over the small coverage of the piconet in DS-UWB system. Based on the simulation, we obtain various performance on the mean acquisition time by varying the parameters, such as the total number of hypotheses to be searched, subgroup size, and dwell time. Then, we suggest the optimum parameter set for the initial acquisition in DS-UWB system.

Key Words : DS-UWB System, Acquisition, Detection, Miss and False Alarm

Ⅰ. Introduction

Ultra-WideBand (UWB) technology is the basis for wireless personal area networks (WPAN), intended for the use of the 3.1- 10.6 GHz of unlicensed band subject to the FCC Part 15 rules that specify a maximum transmit power spectral density of -41.3 dBm. UWB schemes can achieve very high aggregate data rates over short distances due to the ultra-wide bandwidths employed.

In this paper, we focus extensively on the issues of initial acquisition in the direct sequence UWB (DS-UWB) system based on the acquisition sequence defined in the IEEE802.15.3a proposal [1]. Compared with other works, we obtain meaningful analytical results on initial acquisition, which is specific to the UWB channel environment in the presence of multiple H_1 cells (in-phase cells) and data modulation in the acquisition sequence. Besides, we present the simulation performance of detection, miss, false alarm probabilities and mean acquisition time under the UWB channel environment. Furthermore, we suggest the optimum number of subgroups and dwell time in search and verification modes through simulation.

This paper is organized as follows. In section 2, we analyze the specific scenario in the UWB system and derive the detection, miss and false alarm probabilities in search and verification modes in theory. Furthermore, we get the state transfer diagram and analytical mean acquisition time based on the above probabilities. All the analysis we derived is on the basis of double-dwell hybrid acquisition scheme. We present the performance of initial acquisition in the DS-UWB system based on the acquisition sequence defined in the proposal and double-dwell hybrid acquisition scheme in section 3.

Finally, conclusions are made in section 4.

Ⅱ. Analysis on the Performance of Initial Acquisition

2.1 Probability Distribution Function for DS-UWB System

With a large number of multipath components, the complex amplitude of the received signal has a complex Gaussian distribution [2]. Based on the non-coherent detector structure, the decision varaible η, which is the sum of mutually-independent I/Q non-coherent correlator outputs Z_l, l = 1, 2, ···, L, is chi-squared distributed with $2L$ degrees of freedom under hypothesis H_0 or H_1 [3]. H_1 is the in-phase cell and H_0 means the out-phase cell. The probability density function of η under H_0 is as in (1).

* 인하대학교 정보통신대학원 이동통신연구실 (charles535@hotmail.com, khchang@inha.ac.kr),
논문번호 : KICS2006-04-171, 접수일자 : 2006년 4월 17일, 최종논문접수일자 : 2006년 7월 14일

$$f_\eta(\eta|H_0)=\frac{1}{(L-1)!V_{H_0}^{L}}\eta^{L-1}e^{\frac{-\eta}{V_{H_0}}} \quad (1)$$

where L is the post-detection integration period. Furthermore, we use V_{H_0} to represent the correlator output when the H_0 cell is under test and $V_{H_0}=N_cI_0$. Here, N_c is the spreading factor of the acquisition sequence, and I_0 is the interference spectral density that is caused by the background noise and other interference.

In this paper, we consider there is multiple number of H_1 hypotheses. The probability density function of η under H_1 hypothesis is given by

$$f_\eta(\eta|H_{1,i})=\frac{1}{(L-1)!V_{H_{1,i}}^{L}}\eta^{L-1}e^{\frac{-\eta}{V_{H_{1,i}}}} \quad i=1,\ 2,\ ...,\ I \quad (2)$$

where $V_{H_{1,i}}$ means the output of the I/Q non-coherent correlator when the i^{th} H_1 hypothesis is under test. $V_{H_{1,i}}$ is given in (3), considering the effect of data modulation in the acquisition sequence.

$$V_{H_{1,i}}=N_c^2E_c\sum_{j=1}^{I}d^2(t)\cdot R_d^2(\lceil(\xi_i-\tau_j)/N_c\rceil)\cdot E[\alpha_j^2]\cdot R_c^2(\xi_i-\tau_j)+N_cI_0 \quad i=1,\ 2,\ ....,\ I \quad (3)$$

Here, the acquisition sequence is generated in a manner that a PN sequence is spread by the piconet acquisition code (PAC) [1]. In (3), E_c is the chip energy of PAC, $d(t)$ is the PN sequence to generate the acquisition sequence with normalized autocorrelation function R_d, and R_c is the normalized autocorrelation function of PAC, ξ_i and τ_j are the time information of the i^{th} H_1 hypothesis and j^{th} path, respectively. Both the time information are normalized to one chip period T_c of PAC.

According to the IEEE 802.15.SG3a final channel report [4], we have

$$\sum_{j=1}^{I}E\left[\alpha_j^2\right]=\sum\Omega_0e^{-T_l/\Gamma}e^{-\tau_{k,l}/\gamma} \quad (4)$$

where Ω_0 is the mean energy of the first path of the first cluster, T_l is the arrival time of the first path of the l^{th} cluster, $\tau_{k,l}$ is the delay of the k^{th} path within the l^{th} cluster relative to arrival time T_l of the first path. Γ and γ are the cluster and ray decay factor, respectively. For simplicity, we can convert (3) to (5) based on (4) with the assumption that the PN sequence used to generate the acquisition sequence is orthogonal.

$$V_{H_{1,i}}=N_c^2E_c(\sum\Omega_0e^{-T_l/\Gamma}e^{-\tau_{k,l}/\gamma})\left\{\sum_{j=1}^{I}R_c^2(\xi_i-\tau_j)\right\}+N_cI_0 \quad \text{where } |\xi_i-\tau_j|\le N_c \quad i=1,\ 2,\ ....,\ I \quad (5)$$

We consider, in this paper, a hybrid acquisition scheme that combines both parallel acquisition and serial acquisition. Besides, the acquisition process consists of search and verification modes. The search and verification processes in hybrid acquisition scheme are shown in Fig. 1, which consists of a bank of N parallel I/Q non-coherent correlators. Uncertainty region V, which is defined as the total hypotheses to be searched, is represented by W/Δ. Here, W denotes the maximum transmission delay according to the piconet coverage, and Δ represents the search step size. Both W and Δ are normalized to one chip period of PAC.

Then, we partition the uncertainty region V into Q subgroups for the hybrid acquisition. Q becomes V/M, where M is the number of hypotheses in one subgroup. In this paper, H_1 subgroup means the subgroup which contains at least one H_1 hypothesis. However, H_0 subgroup is the subgroup which contains no H_1 hypothesis.

Considering the deployment scenario of the abundant multipath components over the small coverage of the piconet in DS-UWB system, there is very larger number of H_1 hypotheses compared with the case of

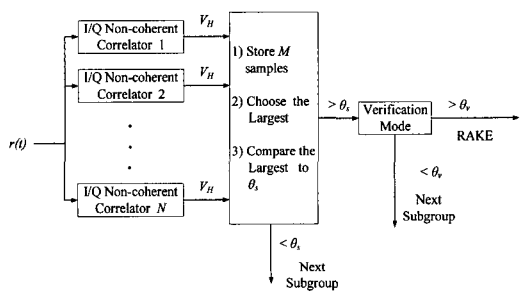

Fig. 1. Search and verification processing in hybrid acquisition scheme.

the conventional CDMA system. In addition to that, the multipath components are scattered over the most part of the uncertainty region under UWB channel environments, so it is not practical to set the large subgroup size to contain all H_1 hypotheses in one or two subgroups as in the conventional CDMA system of [5]. In this paper, we assume there are n number of H_1 subgroups which contains H_1 hypotheses. The value of n depends on the number of H_1 hypotheses and the subgroup size M. We also assume that the i^{th} H_1 subgroup will contain I_i number of H_1 hypotheses.

2.2 Detection, Miss and False Alarm Probabilities in Search and Verification Modes

In this section, using (1)-(5) we derive the detection, miss and false alarm probabilities in search and verification modes, respectively.

The detection probability $P^i_{d_{s,j}}$ in search mode, for the jth H_1 hypothesis in the ith H_1 subgroup is defined in this paper as the probability that the correlation value at the j^{th} H_1 hypothesis is larger than the values at the other (M-1) hypotheses in the subgroup and the detection threshold Θ_s of the search mode. We represent $P^i_{d_{s,j}}$ as

$$P^i_{d_{s,j}} = \int_{\theta_s}^{\infty}\Big[f_\eta(\eta|H_{1,j})\,\{\int_0^{\eta} f_x(x|H_0)\,dx\}^{M-I_i} \cdot \prod_{\substack{l=I_{i-1}+1 \\ l\neq j}}^{I_i}\{\int_0^{\eta} f_y(y|H_{1,l})\,dy\}\,d\eta\Big] \quad i=1,\,2,\,...,\,n \quad j=I_{i-1}+1,\,...,\,I_i \tag{6}$$

Then, the detection probability $P^i_{d_s}$ in search mode for the i^{th} H_1 subgroup is given as

$$P^i_{d_s} = \sum_{j=I_{i-1}+1}^{I_i} P^i_{d_{s,j}} \quad i=1,\,2,\,...,\,n \tag{7}$$

The miss probability $P^i_{m_s}$ in search mode for the i^{th} H_1 subgroup is defined as the probability that all the correlation values in the i^{th} H_1 subgroup are less than Θ_s.

$$P^i_{m_s} = \prod_{j=I_{i-1}+1}^{I_i}[\int_0^{\theta_s} f_\eta(\eta|H_{1,j})\,d\eta][\int_0^{\theta_s} f_\eta(\eta|H_0)\,d\eta]^{(M-I_i)} \quad i=1,\,2,\,...,\,n \tag{8}$$

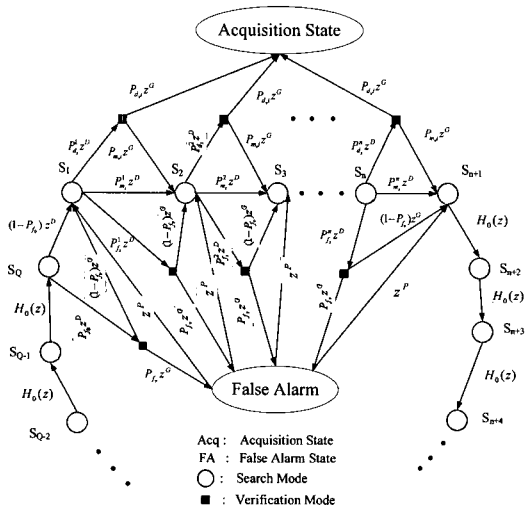

Fig. 2. State transfer diagram for hybrid scheme.

The false alarm probability $P^i_{f_s}$ in search mode for the i^{th} H_1 subgroup is given by

$$P^i_{f_s} = 1 - P^i_{d_s} - P^i_{m_s} \quad i=1,\,2,\,...,\,n \tag{9}$$

The false alarm probability P_{f_0} in search mode for the H_0 subgroup is the probability that the correlation values at H_0 hypothesis exceeds the detection threshold Θ_s and is given as following:

$$P_{f_0} = \Big[\int_{\theta_s}^{\infty} f_\eta(\eta|H_0)\,d\eta\Big]^M \tag{10}$$

In verification mode, each hypothesis is tested independently without the concept of subgroup. So the detection probability $P_{d_{v,j}}$ of verification mode is the probability that the correlation value at the H_1 hypothesis exceeds the detection threshold Θ_v and is represented as in (11).

$$P_{d_{v,j}} = \int_{\theta_v}^{\infty} f_\eta(\eta|H_{1,i})\,d\eta \quad i=1,\,2,\,...,\,I \tag{11}$$

The miss in verification mode means a correlation value at the H_1 hypothesis is less than the detection threshold Θ_v. The miss probability $P_{m_{v,j}}$ can be written as

$$P_{m_{v,j}} = \int_0^{\theta_v} f_\eta(\eta|H_{1,i})\,d\eta \quad i=1,\,2,\,...,\,I \tag{12}$$

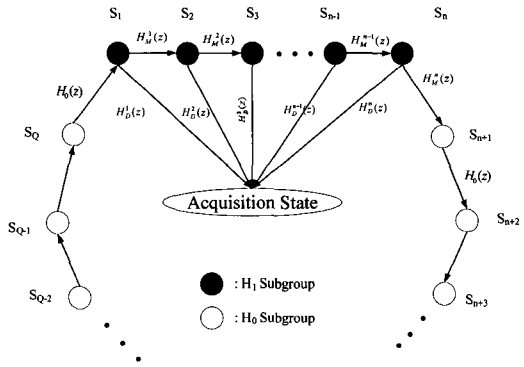

Fig. 3. Simplified state transfer diagram.

The false alarm probability P_{f_v} in verification mode means the probability that the correlation values at H_0 hypothesis exceeds the detection threshold θ_v.

$$P_{f_v} = \int_{\theta_v}^{\infty} f_\eta(\eta|H_0)\, d\eta \tag{13}$$

2.3 Analytical Mean Acquisition Time

The hybrid acquisition system described above can be represented as a state diagram shown in Fig. 2. In this figure, $H_0(z)$ means the state transfer function from the H_0 subgroup to the next subgroup. D is the number of hypotheses that are assigned to a correlator, and G is the ratio of the dwell time in verification mode to the dwell time in search mode. P is the penalty time when false alarm happens.

Fig. 3 is the simplified state transfer diagram of Fig .2. In Fig. 3, $H_D^i(z)$ represents the state transfer function which starts at the i^{th} H_1 subgroup and successfully ends at the acquisition state. $H_M^i(z)$ is the miss-state transfer function which goes from the i^{th} H_1 subgroup to the next subgroup. In both Fig. 2 and Fig. 3, the system searches the subgroups in the clockwise direction. Referring to Fig. 2 and Fig. 3, we can get the state transfer function and finally derive the mean acquisition time (MAT) in theory.

Referring to Fig. 2, we have

$$H_D^i(z) = \sum_{j=I_{i-1}+1}^{I_i} P_{d_{s,j}}^i P_{d_{v,j}} \qquad i = 1, 2, \ldots, n \tag{14}$$

$$H_M^i(z) = P_{m_s}^i z^D + \sum_{j=I_{i-1}+1}^{I_i} P_{d_{s,j}}^i P_{m_{v,j}} z^{D+G} + P_{f_s}^i P_{f_v} z^{D+G+P} + P_{f_s}^i (1-P_{f_v}) z^{D+G} \tag{15}$$

$$H_0(z) = (1-P_{f_0}) z^D + P_{f_0} P_{f_v} z^{D+G+P} + P_{f_0}(1-P_{f_v}) z^{D+G} \tag{16}$$

In Fig. 3, regarding the first H_1 subgroup S_1, the clockwise transfer function from an initial H_0 subgroup to an i-branch apart H_0 subgroup is given by

$$T_i(z) = \frac{(H_0(z))^i H_D^1(z)}{1-(H_0(z))^{Q-n} \prod_{j=1}^{n} H_M^j(z)} \tag{17}$$

The transfer function that starts at the k^{th} H_1 subgroup S_k is represented by

$$T_k(z) = \frac{H_D^k(z)}{1-(H_0(z))^{Q-n} \prod_{j=1}^{n} H_M^j(z)} \tag{18}$$

From (17) and (18), since all subgroups are a priori equally likely, the resultant transfer function averaged over all Q starting subgroups is represented by

$$\begin{aligned} U(z) &= \frac{1}{Q}\left[\sum_{i=1}^{Q-n} T_i(z) + \sum_{k=1}^{n} T_k(z)\right] \\ &= \frac{1}{Q} \frac{H_0(z)[1-(H_0(z)^{Q-n})] H_D^1(z) + [1-H_0(z)] \sum_{k=1}^{n} H_D^k(z)}{[1-H_0(z)][1-(H_0(z))^{Q-n} \prod_{j=1}^{n} H_M^j(z)]} \end{aligned} \tag{19}$$

Thus, the mean acquisition time is given by

$$\begin{aligned} E[T_{ACQ}] &= \frac{d}{dz} U(z)\Big|_{z=1} \cdot \tau_s \\ &= U(z) \frac{d}{dz} \ln U(z)\Big|_{z=1} \cdot \tau_s \\ &= U(z)[A(z) - B(z) - C(z)]\Big|_{z=1} \cdot \tau_s \end{aligned} \tag{20}$$

where τ_s is the dwell time in search mode. The functions of $A(z)$, $B(z)$ and $C(z)$ are given in (21)-(23), where "' " denotes the derivative on z.

$$\begin{aligned} A(z) &= \frac{\mathrm{NUM_A}}{\mathrm{DEN_A}} \\ &\text{where} \\ \mathrm{NUM_A} &= H_0'(z) H_D^1(z)[1-(H_0(z)^{Q-n})] + H_0(z) H_D^{1\prime}(z)[1-(H_0(z)^{Q-n})] \\ &\quad + (n-Q) H_0(z)^{Q-n} H_0'(z) H_D^1(Z) + \sum_{k=1}^{n} [(1-H_0(z)) H_D^{k\prime}(z) - H_0'(z) H_D^k(z)] \\ \mathrm{DEN_A} &= H_0(z)[1-(H_0(z)^{Q-n})] H_D^1(z) + [1-H_0(Z)] \sum_{k=1}^{n} H_D^k(Z) \end{aligned} \tag{21}$$

$$B(z) = -\frac{H_0'(z)}{1-H_0(z)} \tag{22}$$

$$C(z) = -\frac{(Q-n)(H_0(Z))^{Q-n-1} H_0'(z) \prod_{j=1}^{n} H_M^j(z) + (H_0(z))^{Q-n} \sum_{j=1}^{n} [H_M^{j\prime}(z) \prod_{k=1, k\neq j}^{n} H_M^k(z)]}{1-(H_0(z))^{Q-n} \prod_{j=1}^{n} H_M^j(z)} \tag{23}$$

Ⅲ. Validation of Initial Acquisition Performance

In this section, we validate the performance of initial acquisition via detection, miss, false alarm probabilities and mean acquisition time based on the acquisition sequence in DS-UWB system.

The parameters in the simulation are as follows:

- Coverage of the piconet : 10 meters
- Fixed thresholds in search and verification modes
  - Threshold in search mode : 0.15
  - Threshold in verification mode : 0.20
- Acquisition sequence: Nominal preamble structure defined in [1]
- Chip rate of PAC : 1.365 GHz
- Penalty time : 10^6 chip periods
- All the simulations are under UWB channel model (CM) 1 with 100 channel realizations. Here, the number of multipath components is adapted to NP_{10dB}. [4].

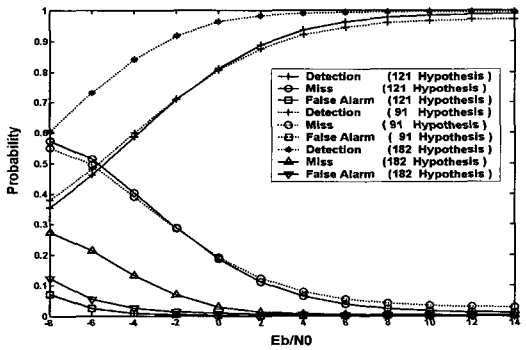

Fig. 4. Detection, miss and false alarm probabilities. 1-chip step size for 91 and 121 hypotheses. 1/2-chip step size for 182 hypotheses.

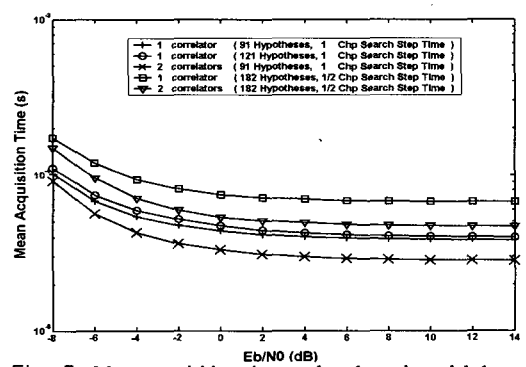

Fig. 5. Mean acquisition time under channel model 1.

In Fig. 4, we present the probabilities of detection, miss and false alarm in different cases of hypothesis number. According to the coverage of piconet, we find that there are total 91 hypotheses with one-chip step size for search, that is, 182 hypotheses with half-chip step size. Furthermore, we consider the case that when the receiver is located at the boundary of the piconet, some H_1 hypotheses might be out of the uncertainty region according to the multipath profile. So we extend the uncertainty region up to 121 hypotheses to contain all the H_1 hypotheses existing. From Fig. 4, after the extension of the uncertainty region, we observe better detection and miss probabilities, while the false alarm probability is nearly the same. Comparing the case of one-chip search step size with the case of half-chip search step size, we find that the probabilities of detection and miss with half-chip step size are much better. However, the false alarm probability with half-chip step size is worse for low E_b/N_0.

In Fig. 5, we show the performance of mean acquisition time in the cases of different search step size, number of correlators and uncertainty region. We see that the mean acquisition time is relative to the number of hypotheses, i.e., the larger the number of hypotheses, the longer the mean acquisition time. Mean acquisition time, of course, becomes larger for the case of the extension of the uncertainty region. Smaller step size and the number of correlators also increase the mean acquisition time.

Fig. 6 shows the MAT performance of DS-UWB system when the hypotheses are divided into different number of subgroups. From the simulation results, we find that the MAT performance is similar when the hypotheses are divided into 2 or 3 subgroups. The optimum MAT performance is obtained when there are 2 or 3 subgroups depending on E_b/N_0, that is, one subgroup will cover the interval of 45 or 30 chips, respectively.

We show MAT performance by varying the dwell time for search and verification modes. From Fig. 7, we get the minimum MAT when we use 2 symbols for search mode and 512 symbols for verification mode, i.e., the whole length of the acquisition sequence.

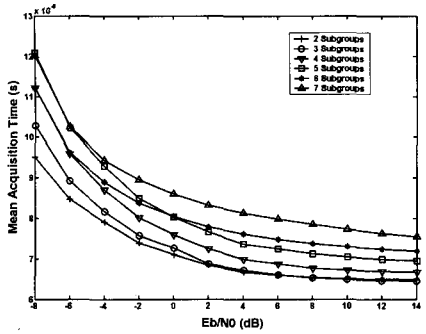

Fig. 6. Mean acquisition time with the different number of subgroups under CM 1.

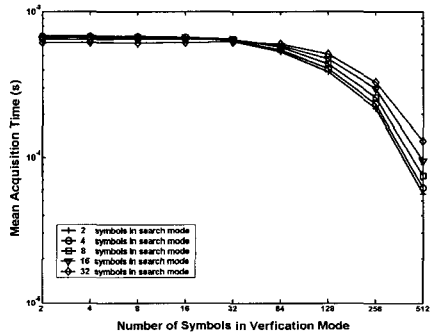

Fig. 7. MAT with the different dwell time in search and verification modes with -8 dB Eb/N0 under CM 1.

Ⅳ. Conclusions

In this paper, we analyze the detection, miss, false alarm probabilities of DS-UWB system in search and verification modes, and the mean acquisition time. Then, we validate the performance of initial acquisition in DS-UWB system through simulation. The increase on the number of H_1 hypotheses will increase the detection probability and reduce the miss probability in both modes. On the other hand, the increase on the number of H_0 hypotheses will increase the false alarm probability. Even though the extension of uncertainty region achieves better detection and miss probabilities, this improvement does not result in the improvement on the mean acquisition time due to the increased number of hypotheses. So the extension of uncertainty region to contain all the H_1 hypotheses is not recommended. Based on the above comparison on MAT performance, we propose the subgroup size of 30 or 45 chips depending on E_b/N_0 and the dwell time of 2 and 512 symbols for search and verification modes, respectively.

References

[1] Reed Fisher, Ryuji Kohno, Michael Mc. Laughlin and Matt Welborn, DS-UWB Physical Layer Submission to 802.15 Task Group 3a, IEEE P802.15-04/0137r4, Jan. 2005.

[2] Andreas F. Molisch and Jeffrey R. Foerster, "Channel models for ultrawideband personal area networks," *IEEE Wireless Communications*, vol. 10, issue 6, pp. 14-21, Dec. 2003.

[3] Athanasios Papoulis and S. Unnikrishna Pillai *Probability, Random Variables and Stochastic Process*, McGraw-Hill, Avenue of Americas, New York, NY 10020, U.S.A, 2002.

[4] Jeff Forster, Sub-committee Chair, Channel Modeling Sub-committee Report, IEEE P802.15-02/490r1-SG3a, Feb. 2003.

[5] Bub-Joo Kang, Hyung-Rae Park and Youngnam Han, "Hybrid acquisition in DS/CDMA forward link," in *Proc. IEEE 47th Veh. Tech. Conf. - Spring*, vol. 3, May, 1997, pp. 2123 - 2127.

왕 우 붕 (YuPeng Wang) 준회원

2004년 7월 동북대학교 통신공학과 (공학사)

2004년 9월~현재 인하대학교 정보통신대학원 석사과정

<관심분야> 4세대 이동통신 시스템, UWB 시스템 무선 전송규격

장 경 희 (KyungHi Chang) 종신회원

1985년 2월 연세대학교 전자공학과 (공학사)

1987년 2월 연세대학교 전자공학과 (공학석사)

1992년 8월 Texas A & M Univ., EE Dept. (Ph.D.)

1989년~1990년 삼성종합기술원 주임연구원

1992년~2003년 한국전자통신연구원, 이동통신연구소 무선전송방식연구팀장 (책임연구원)

2003년~현재 인하대학교 정보통신대학원 부교수

<관심분야> 4세대 이동통신 및 3GPP LTE 무선전송방식, WMAN 및 DMB 시스템 무선전송기술, Cognitive Radio, Cross-layer Design